Section 3: Methods for studying the function, modulation and reorganisation of the human sensorimotor system

Imaging techniques can provide powerful methods for investigating functional-anatomical systems in the human brain. All of the experiments in this thesis use functional magnetic resonance imaging (FMRI) to quantify brain activation patterns associated with sensory or motor tasks in normal subjects or stroke patients. In addition to providing relatively high spatial resolution, FMRI has the advantage of not requiring use of ionising radiation and so is suitable for longitudinal studies which can be crucial in monitoring recovery processes. This section describes some of the general principles of FMRI and methodological considerations specific to the scope of this thesis. The final experiments in this thesis (Section 9) additionally used the technique of transcranial magnetic stimulation (TMS). TMS can be used as a temporary interference technique and therefore allows one to test the hypothesis that activation of a specific brain area is crucial for performance of a particular task. This section also describes some of the principles of TMS.

3.1 Functional Magnetic Resonance Imaging (FMRI)

Use of FMRI has increased exponentially in the decade following the first publication using FMRI to demonstrate visual activation in human subjects (Belliveau *et al.* 1991). It is now the tool of choice for many neuroscientists investigating systems-level functional anatomy in normal or clinical populations. As a method to quantify brain activation it has many advantages over the older technique of positron emission tomography (PET). These include improved spatial and temporal resolution, and the ability to perform repeated measurements safely on the same subjects.

3.1.1 Physical principles of Magnetic Resonance

Nuclei that have an odd number of nucleons possess a magnetic moment and a spin (Figure 3.1a). When such nuclei are placed in an external magnetic field the intrinsic magnetic moment and spin cause the nuclei to precess about the axis of the static field (Figure 3.1c). The nuclear spins align parallel or anti-parallel to the external field with a majority of the

particles aligned parallel to the field as this is the lower energy state. This creates a net magnetization in the direction of the static field. The protons oscillate about the axis of the static field with a frequency (the Larmor frequency) determined by the strength of the field and the gyromagnetic ratio of the proton (fixed for each nucleus).

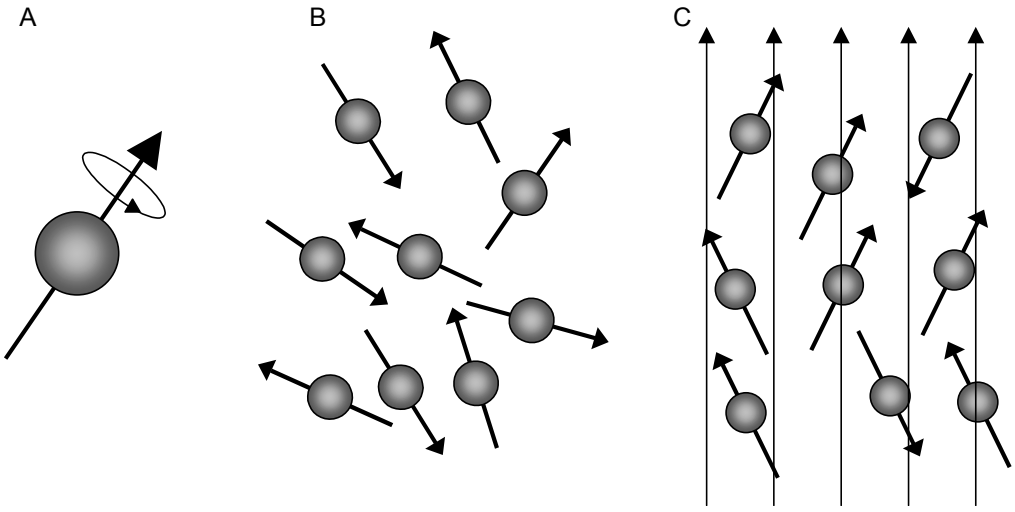

Figure 3.1: A: A proton with a magnetic moment precessing about its own axis. **B:** Randomly aligned protons in the absence of an external magnetic field. **C:** When the external magnetic field is applied the majority of spins align parallel to the field, creating a net magnetization in the direction of the applied field.

In MRI we are typically interested in hydrogen nuclei in water. When the head is placed inside a strong magnetic field the hydrogen protons precess about the axis of the external field and align parallel or anti-parallel with it (the z direction). A radiofrequency (RF) pulse is transmitted to the subject from a surrounding transmitter coil. If the frequency of the RF pulse matches the Larmor frequency of the precessing protons then resonance occurs, i.e. energy is transferred to the spins. In a classical model, this can be conceptualised as the protons being 'flipped' away from the direction of the static field (Figure 3.2). The angle by which the spins are flipped depends on the strength and duration of the RF pulse. For example, a 90° pulse will flip the net magnetisation vector into the plane perpendicular to the direction of the static field (the x-y direction). The oscillating RF pulse causes the

protons to precess in phase about the x-y field, resulting in a transverse component to the net magnetisation that generates an electrical signal in a surrounding receiver coil.

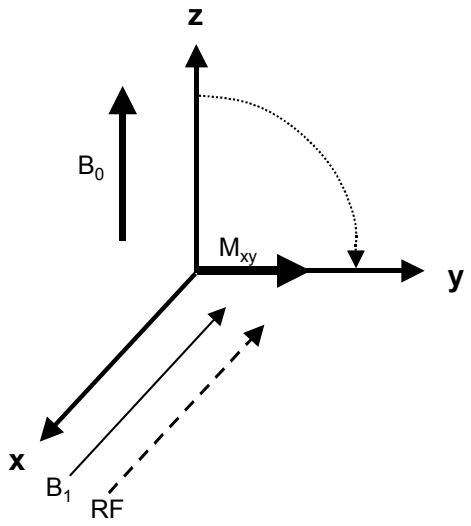

Figure 3.2: After transmission of an RF pulse, the net magnetisation vector is 'flipped' away from the axis of the static magnetic field (B_0), towards the xy plane. In this example the vector is flipped by 90°, resulting in the entire magnetisation vector ending up in the xy plane (M_{xy}). The magnetic field associated with the RF pulse is labelled B_1. The strength of B_1, and the duration of the RF pulse, determines the angle by which the magnetisation vector is flipped. Figure based on (Hashemi and Bradley 1997)

3.1.1.1 Generating contrast

There are various ways in which contrast can be generated in an MR image (Figure 3.3). First, it is possible simply to image the density of protons of interest. If MR signal is acquired immediately after an RF pulse then the MR signal is maximum as the maximum number of spins will still have magnetisation in the x-y plane (where signal can be detected). If in addition the time between RF pulses is long enough for the magnetization to have realigned with axis of the external field (and so maximum magnetization is available to be flipped) then a signal acquired immediately after an RF pulse will reflect proton density.

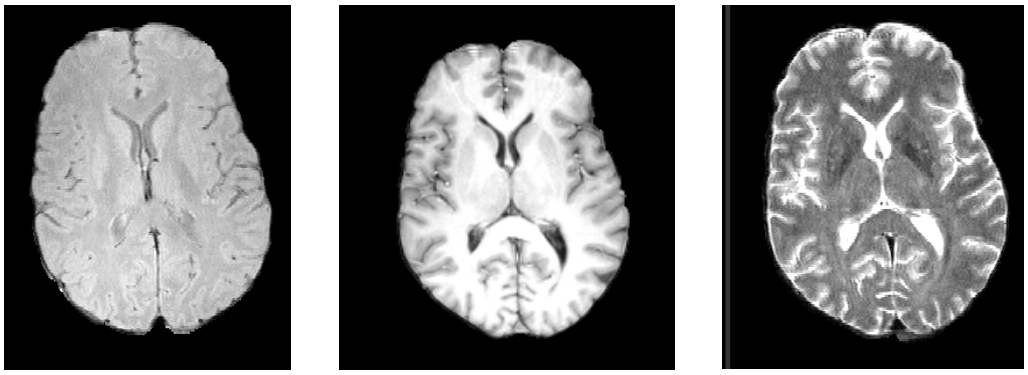

Figure 3.3: Examples of proton density image (**left**), T1-weighted image (**centre**) and T2-weighted image (**right**)

However, if the MR signal is acquired at some delay from the RF pulse, then there will have been some decay in the MR signal. After an RF pulse two separate processes occur: there is a recovery of longitudinal (z) magnetisation (in the direction of the static field) and there is a decay in transverse (x-y) magnetisation. These two processes provide further sources of contrast in MR imaging and are described by their time constants – T1 and T2.

After an RF pulse spins realign with the static field at a rate given by T1, the longitudinal relaxation time (or spin-lattice relaxation time). T1 recovery occurs because individual spins revert back to their lowest energy state (i.e. aligned with the static field) and so give up energy to the surrounding environment or 'lattice'. In addition, after an RF pulse a separate process occurs: the magnetisation in the transverse plane decays at a rate given by T2, the transverse relaxation time (or spin-spin relaxation time) (faster than T1). T2 decay occurs because of interactions between spins: spins create their own small magnetic fields which slightly affect their neighbours. This inherent inhomogeneity in the magnetic environment causes dephasing of the spins and a resulting decrease in the net transverse magnetisation. T1 and T2 values are fixed for a given nucleus in a given environment. Therefore, by varying the scan repeat time (TR) and the time between transmitting an RF

pulse and measuring a signal (TE), the contrast between different tissue types is altered (Figure 3.4).

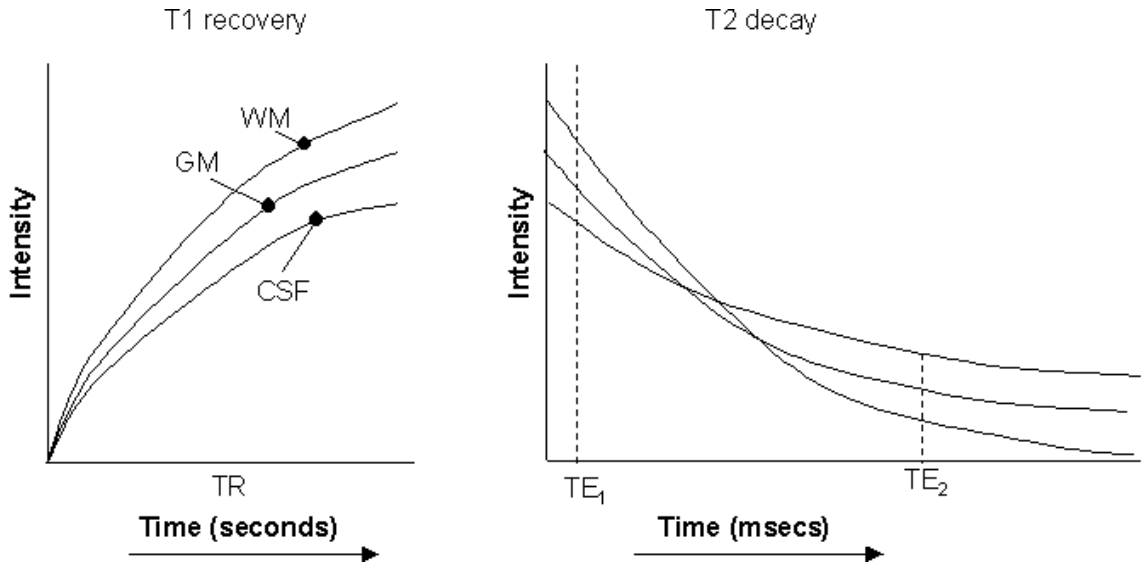

Figure 3.4: T1 recovery and T2 decay curves for white matter (WM), grey matter (GM) and cerebrospinal fluid (CSF). The choice of TR and TE will determine which tissue types show up bright or dark on the image. Note the different time scales of the two graphs – the timescale of TR (typically seconds) is far greater than TE (typically tens of milliseconds). The degree of T1 recovery that has occurred after an RF pulse will determine how much longitudinal magnetization is available to be flipped by the following RF pulse. If nearly complete T1 recovery is allowed to occur after an RF pulse (i.e. TR is long) and a signal is acquired very quickly after the next RF pulse (i.e TE is short) then intensity will depend on proton density (not shown). However, if TR is short and TE is short (e.g. TE_1 in this figure), then intensity will depend on the T1 recovery times of the different tissue types. Therefore, in a T1-weighted image white matter is bright, grey matter is intermediate and CSF is dark. If TE is long (e.g TE_2 in this figure) then intensity will depend on the T2 decay of the different tissue types. Therefore, in a T2-weighted image CSF is bright, grey matter is intermediate and white matter is dark.

A third decay parameter, T2* also characterises the rate of decay of transverse magnetisation but is dependent on field inhomogeneities as well as tissue type and magnetic field strength. Local inhomogeneities cause further dephasing of the spins and therefore T2* is shorter than T2. When the receiver coil detects the current induced by transverse magnetisation after an RF pulse, it will receive an oscillating current which decays over time with a rate given by T2*.

3.1.1.2 Encoding spatial information

Spatial information about the source of the signal is provided by three orthogonal gradient coils (Gx, Gy, Gz). Each gradient coil generates a small (e.g. 25-40mT/m) spatially varying magnetic field along one axis that is superimposed on the large static magnetic field (e.g. 1.5 – 3T). By convention, z refers to the axis along the length of the magnet bore. If a subject is lying supine along the length of the bore then the x refers to the axis from ear to ear and y refers to the axis from the front to the back of the head. In the case of axial slice acquisition, Gz allows for slice selection as protons at different points along the gradient will precess at different frequencies, and only those protons whose frequencies are matched by the RF pulse will be flipped. Therefore the RF pulse is applied at a range of frequencies (bandwidth) designed to flip protons at a particular range of spatial locations along the z-axis. The x and y gradients allow for spatial coding within a slice. Gx ('frequency-encode gradient') causes protons at different locations along the x axis to precess at different frequencies. Gy ('phase-encode gradient') causes protons at different points along the y axis to have a different phase. Thus, each x,y pixel within a slice has a unique frequency and phase that encode the spatial location of the pixel.

3.1.1.3 Data space and image reconstruction

The signal from each slice is received in frequency space, or k-space (Figure 3.5). The frequency information is reconstructed into an image using a Fourier transform. With most pulse sequences a single line of k-space is sampled after each RF pulse. However, the newer technique of echo planar imaging (EPI) uses very rapidly switching gradients to enable sampling of the whole of k-space after a single RF pulse (Figure 3.6). This enables much faster scanning, and is often employed in functional MRI studies.

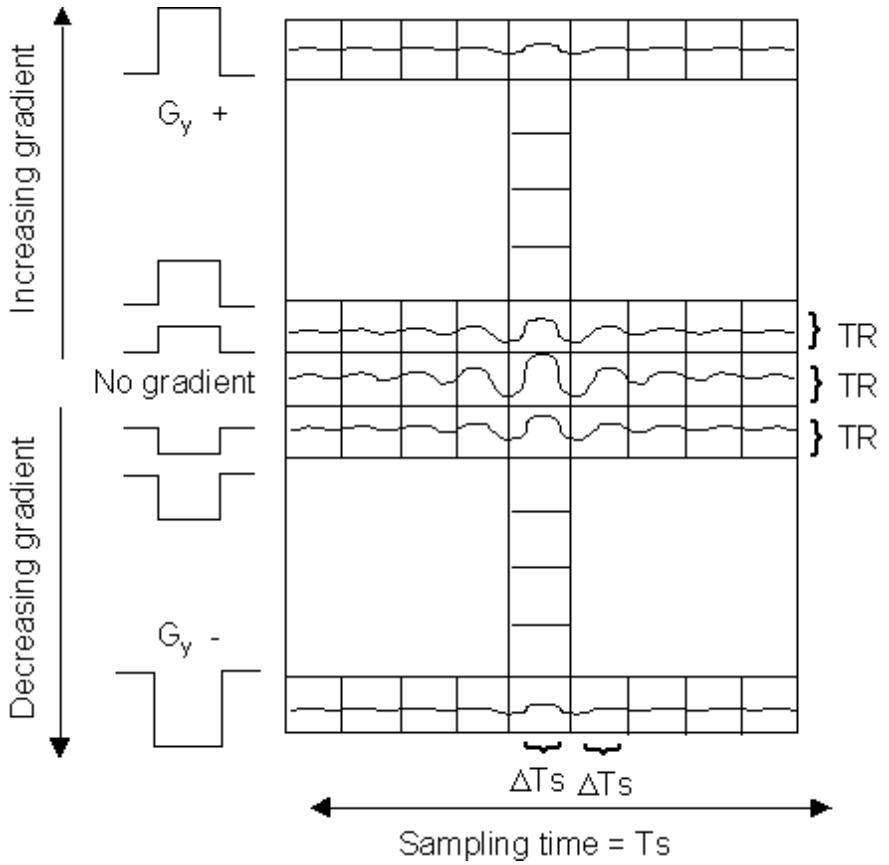

Figure 3.5: MRI data is acquired in frequency space, or k-space. The data from a spin echo experiment can be represented in analogue form as a series of signals (echoes). One row of k-space represents the signal acquired across a whole slice during a single TR. There are as many rows of k-space as there are phase-encoding steps. Each phase-encoding step is gathered with a different phase-encode gradient (Gy). The central row of k-space represents data acquired with no phase-encode gradient. Rows below this are acquired with increasingly negative phase-encode gradients ands rows above it with increasingly positive gradients. Applying phase-encode gradients causes dephasing of the signal and therefore rows above and below the centre of k-space are smaller in amplitude than the central row. Each row of k-space represents a single echo signal. The peak of the echo is in the centre of the row. Towards the edges of a row the signal has not yet reached maximum (to the left of centre) or is dephasing (to the right of centre) and so is reduced in amplitude. Therefore the maximum signal intensity is found in the centre of k-space. The periphery of k-space has low intensity signal but contains information about fine detail in the reconstructed image. Figure based on (Hashemi and Bradley 1997)

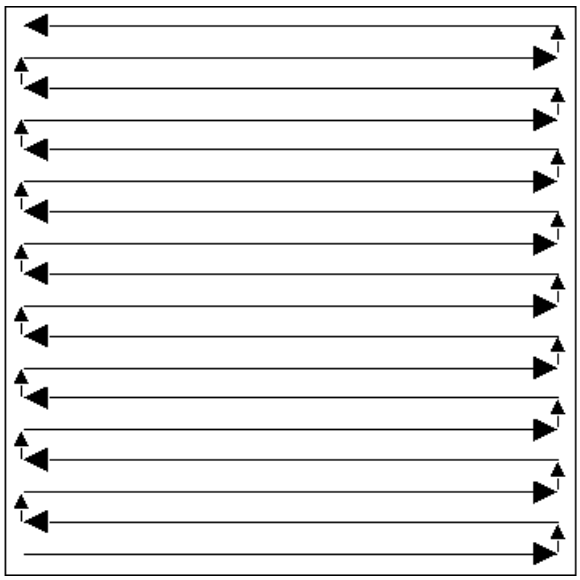

Figure 3.6: In single shot Echo-Planar Imaging (EPI) the whole of k-space is acquired after a single RF pulse. This requires rapid switching of the frequency-encode gradient (Gx) from negative to positive (to move backwards and forwards along rows of k-space) and 'blipping' of the phase-encode gradient (Gy) to move up to the next row of k-space.

3.1.2 Physiological principles of BOLD imaging

The fact that T2* decay reflects local magnetic field inhomogeneities is exploited by functional MRI as local inhomogeneities can reflect functionally relevant changes. This was first established by injection of the paramagnetic contrast agent, gadolinium-DTPA, into the blood stream. As the contrast agent travels through blood vessels it causes local increases in magnetic susceptibility around the vessels that results in local loss of signal depending on the amount of contrast agent present. The first functional MRI study of the human brain used this technique to detect increases in blood volume in visual cortex during photic stimulation (Belliveau *et al.* 1991).

The need for exogenous contrast agents was removed by the discovery that local changes in MR image contrast arise simply from changes in blood oxygenation as deoxyhaemoglobin (deoxy-Hb) is more paramagnetic that oxyhaemoglobin (oxy-Hb) (Ogawa *et al.* 1990). When oxygen intake is modulated in experimental animals, the ratio of

oxy-Hb to deoxy-Hb changes, causing a change in magnetic susceptibility around the vessels, and a resultant change in MR signal.

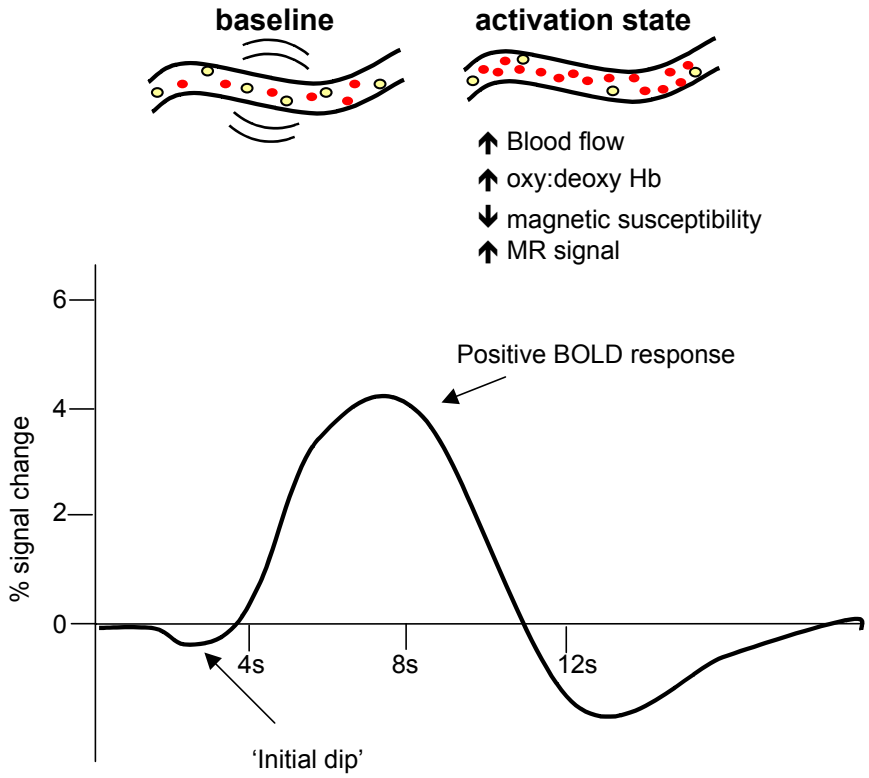

Figure 3.7: The BOLD response. In the baseline state (top left) there is distortion of the magnetic field around a blood vessel. With increased neuronal activity (top right) there is an increase in blood flow greater than the increase in oxygen consumption, resulting in an increase in the ratio of oxy- to deoxy-Hb. This results in a decrease in magnetic susceptibility around the vessel and therefore an increase in FMRI signal. The positive BOLD signal is delayed by 4-6 seconds (graph, bottom) from the onset of neuronal activity. However, there are also reports of a brief, negative BOLD signal (the negative dip) possibly reflecting an initial decrease in the ratio of oxy- to deoxy-Hb.

Changes in blood oxygenation also occur as a result of neuronal activity and so the BOLD signal can be used as an indirect marker of cellular firing. Neuronal activity results in high metabolic demand, which is largely met by increased oxidative metabolism. Extra oxygen is supplied by increased local blood flow. The increase in blood flow is largely due to increased blood velocity rather than increased blood volume. The increase in blood flow exceeds the increase in oxygen consumption. Thus, the ratio of oxy-Hb to deoxy-Hb increases in areas of increased neuronal activity. Reduction in the concentration of

paramagnetic deoxy-Hb results in reduced magnetic susceptibility around the vessels, and thus higher MR signal (Figure 3.7).

Explanations for the mismatch between oxygen consumption and blood flow include the oxygen limitation model (Buxton *et al.* 1998). This model holds that oxygen transfer into brain tissue is limited by diffusion from capillaries and depends largely on the oxygen concentration gradient between the vasculature and the tissue. The gradient can be made steeper by increasing blood flow over and above oxygen consumption. Thus the mismatch between blood flow and oxygen extraction would meet the increased oxygen transport demand. An alternative explanation is the suggestion that there is a transient switch to non-oxidative metabolism during neuronal activity (Magistretti and Pellerin 1999). There is evidence that glutamate released at the synapse is taken up by astrocytes triggering increased glucose uptake from capillaries. The glucose is metabolized glycolytically into lactate which is then oxidized by neurons. This series of events would therefore be reflected by an initial mismatch between blood flow and oxygen consumption followed by later recoupling of the two. The initial mismatch would result in the increase in deoxy-Hb detected by BOLD imaging. However, there are suggestions that the existence of the mismatch varies between different cortical areas (Gjedde 1997). For example, certain types of stimulation (e.g. flashing visual checkerboard) have been shown to produce similar increases in blood flow and oxygen consumption in visual cortex (Marrett *et al.* 1993). The difference between this coupling and the more frequently reported mismatch between flow and oxygen consumption may reflect differences in metabolic processes between areas with high and low oxidative capacity(Gjedde 1997).

Some optical imaging studies have shown that immediately after stimulation there is a transient increase in deoxy-Hb (Malonek and Grinvald 1996). This may correspond to the

'initial dip' in BOLD signal that has been detected in some FMRI studies (Menon *et al.* 1995) (Figure 3.7) though the latter finding is somewhat controversial (Villringer 1999)

BOLD signal changes with neuronal activity are small, typically in the order of 2-5%. T2* relaxation rate, and therefore the size of signal detected, is dependent on magnetic field strength. For the same scanning parameters, the signal change at 4T is up to four times larger than at 1.5T (Turner *et al.* 1993).

3.1.3 Spatial resolution of FMRI

There is debate over the degree to which the location of measured BOLD signal changes corresponds to the location of neuronal activity. A number of factors could influence spatial resolution. The theoretical limit to spatial resolution in FMRI is determined by the size of the smallest vascular component that is able to act as an independent functional unit. There is debate over whether this is the capillary or the feeding arteriole. The actual spatial resolution of a study is determined by factors including contrast to noise, amount of motion (from head and brain in cardiorespiratory cycle), the contribution of large vessel effects, and the location and extent of metabolic and haemodynamic changes that occur with neuronal activation. The following sections outline the effects of some of these factors and ways in which their influence can be minimised.

3.1.3.1 Large vessel effects

Sensitivity to haemodynamic changes in large vessels such as draining veins or inflowing vessels have the potential to skew spatial localisation away from capillaries which are close to the site of neuronal activity (Lai *et al.* 1999). Changes around large vessels are likely to be of a greater magnitude than changes around the microvasculature feeding the active tissue (Gati

et al. 1997; Segebarth *et al.* 1999). This can be a particular problem in studies with low signal to noise (e.g., at low field strength) when only large signal changes would be detectable. It can be argued that draining veins would not contribute significantly to the BOLD signal, as the oxygenation change associated with neuronal activation would be substantially diluted more than a few millimetres downstream of the activated area (Lai *et al.* 1999). However, the common empirical finding of 'activation' of remote draining veins such as the saggital sinus suggest that dilution effects are outweighed by the increase in signal magnitude in vessels that occupy large volumes of voxels (Menon and Goodyear 1999).

3.1.3.2 Location and extent of haemodynamic and metabolic changes

Locally increased blood flow at sites of neuronal activity typically reflects increased metabolic demand. Increased metabolism after activity has been localised to the synapse rather than the cell body. It is thought that glutamate reuptake by sodium-dependent transporters on astrocytes surrounding synapses may be a major component of the metabolic demand (Magistretti and Pellerin 1999).

The spatial specificity with which one can detect haemodynamic and metabolic changes in vivo has been investigated using optical imaging of ocular dominance columns in monkeys and cats (Malonek and Grinvald 1996). Unilateral visual stimulation produced neuronal activity in columns corresponding to the stimulated eye. A few seconds after the neuronal activity there was a transient increase in deoxy-Hb. Although the magnitude of this change was greatest over active columns, it also extended over inactive areas. The initial increase in deoxy-Hb was followed by a longer lasting decrease that had even less spatial specificity. The change in CBV (a delayed increase) was also detected over both active and inactive columns and spread even further than changes in deoxy-Hb. These results suggest

that changes in oxygen extraction and, to an even greater extent, changes in blood flow, are not restricted to areas of increased excitatory neuronal activity. This could indicate that the cerebral vasculature "waters the garden for the sake of a single flower", or it could indicate that inhibitory synaptic activity occurring in ocular dominance columns for the unstimulated eye is also metabolically demanding (see Section 3.1.6.1)

3.1.3.3 Strategies for improving spatial resolution

Approaches to reducing large vessel effects include using higher field strengths, surface coils or flow sensitization gradients (Kim *et al.* 1999).

T2* effects increase with increasing field strength. However, biophysical modelling of the BOLD response suggests that the increases are linear for large (>8μm) vessels and greater than linear for small vessels (Ogawa *et al.* 1993). This suggests that the relative contribution of capillaries to the observed signal will increase with increasing field strength.

The influence of large vessels depends also on the imaging sequence chosen. Spin echo techniques are mainly sensitive to changes around small vessels, whereas gradient echo sequences are sensitive to changes around large and small vessels (Ogawa *et al.* 1993).

A potentially exciting approach to maximising spatial resolution within the physiological constraints of BOLD imaging is to map the initial dip in signal, thought to correspond to an early increase in oxygen extraction during neuronal activation (Vanzetta and Grinvald 1999). Comparisons between activation maps derived from the initial dip versus conventional maps of the delayed increase in deoxy-Hb reveals that the initial dip is more precisely localised, at least in anesthetized cats imaged at very high field strength (Kim *et al.* 2000; Duong *et al.* 2000). Although there have been some demonstrations of successful mapping of the initial dip in humans (Hu *et al.* 1997), detection of the dip depends on high

magnetic field strength and fine temporal resolution. Moreover, the magnitude of the negative response is small (1-2%).

A successful alternative approach to improving spatial resolution has been to compare activation patterns in different tasks designed to activate overlapping regions but to different degrees. The rationale is that even if adjacent cortical areas drain into common veins, causing large overlapping areas of apparent activation, there will nevertheless be a small component of the activation unique to neuronal activity in each region (i.e., the signal around local microvasculature). This approach was taken in an elegant FMRI study of ocular dominance columns in human subjects (Menon *et al.* 1997). Visual stimulation of the left or the right eye activated overlapping voxels in visual cortex but identifying those voxels that were activated more by left than right eye stimulation and vice versa the authors were able to map out interleaved ocular dominance columns.

3.1.4 Temporal resolution of FMRI

There is typically a 4-6 second lag between the onset of a stimulus and the peak of the haemodynamic response curve (Figure 3.7). As long as the shape of the haemodynamic response can be accurately estimated then the lag does not need to dictate the useful temporal resolution of the technique, as the expected time course can simply be convolved with the expected haemodynamic response function (HRF). However, there is evidence that the haemodynamic lag varies between individuals (Aguirre *et al.* 1998), cortical areas and task (Rajapakse *et al.* 1998) and with disease (Pineiro *et al.* 2002). It is therefore the *variability* in haemodynamic response latency rather than the lag itself that limits the temporal resolution of FMRI (Bandettini 1999).

Temporal resolution in FMRI is dependent on the repetition time (TR) between acquisitions of signal from the same slice. The choice of TR depends somewhat on T1 recovery time as it is preferable to allow long enough for sufficient recovery of longitudinal magnetisation to take place before the next RF pulse (Figure 3.4). Therefore TR should be longer than T1 (i.e. at least 1- 1.5 seconds). The limits of temporal resolution are also dependent on scanner hardware. If TR is short and multiple slices are acquired then very rapid gradient switching is required.

The importance of temporal resolution of FMRI depends somewhat on the paradigm design chosen. For example, a conventional block design where task blocks of 20-40 seconds duration alternate with rest blocks assumes a constant response across the whole block (once the box car design has been convolved with the HRF). However, in an event-related design the goal is to detect individual responses to single events separated in time (see Figure 3.8). The upper limits of temporal resolution therefore apply largely to event-related designs. As the experiments in this thesis used only conventional block designs (see Section 3.1.7.4) the issues relating to optimal paradigm design for maximal temporal resolution are not discussed here (for reviews see (Friston *et al.* 1999; Buckner 1998)).

3.1.5 Neurovascular coupling

Interpretation of most FMRI studies rests on the assumption that the BOLD signal is an indirect marker of excitatory neuronal activity. However, BOLD signal change is a summary value that could reflect a number of different processes.

3.1.5.1 Excitation or inhibition?

The BOLD signal is typically interpreted as a reflection of excitatory neuronal activity, but to what extent does inhibitory synaptic activity result in increased metabolic demands and thus an increase in the BOLD signal? Studies using 2-deoxyglucose have shown that even purely inhibitory synaptic activity in cat superior olive may result in increased local metabolism (Nudo and Masterton 1986). However, a theoretical argument can be made that inhibitory synaptic activity should have little direct impact on the BOLD signal. The argument rests on the following facts: only 15-30% of neurons are inhibitory; inhibitory cells make fewer synapses than excitatory cells; inhibitory synapses have a strategically better location on the cell, and would therefore operate more efficiently and chloride transport uses less energy that the metabolically-demanding sodium pump (Waldvogel *et al.* 2000). However, theoretical arguments would also suggest that even if inhibitory activity does not lead directly to increased metabolic demand, increasing inhibitory 'tone' will increase the amount of excitatory activity necessary to achieve a given firing rate.

Nevertheless, there is indirect evidence to support the argument that inhibition does not contribute significantly to the BOLD signal. A recent study showed that during tasks for which TMS investigation suggests that inhibitory activity is occurring in M1 (the "no-go" periods of a go, no-go task) no increase in BOLD signal is detected in M1 (Waldvogel *et al.* 2000).

3.1.5.2 Spiking or subthreshold activity?

Recently, direct evidence on the relationship between electrical activity and BOLD signal has been provided by a series of technically impressive studies by Logothetis and colleagues. Logothetis et al performed simultaneous electrophysiological recording and FMRI scanning during visual stimulation in anaesthetized macaque monkeys (Logothetis *et al.* 2001). They compared the haemodynamic response to electrode measurements that were filtered to differentiate high and low frequency components. High frequency (300-1500Hz) components represented single and multi unit activity. Low frequency (40-130Hz) components represented local field potentials (LFPs). LFPs reflect spiking and subthreshold integrative processes whereas multi-unit recordings reflect only spiking. Although both multi-unit activity and LFPs correlated with BOLD signal, LFPs were a significantly better predictor of BOLD response. This was partly due to the fact that one quarter of the multi-unit recordings showed a transient response, with an initial increase in amplitude followed by a return to baseline. By contrast, LFPs (and BOLD signal) displayed a sustained response for the duration of the visual stimulation.

The tight relationship between BOLD and LFPs suggests the signal measured in FMRI reflects input and local processing of an area rather than its spiking output. Thus areas active during performance of a particular task in an FMRI experiment may not correspond to areas shown to be involved in the same task in a single unit recording study. Interpretation of areas of FMRI activation should be guided by knowledge of the connectivity of areas of interest as locally increased BOLD signal may reflect increased firing in a separate area with excitatory projections to the region with increased BOLD signal.

These findings are consistent with the fact that whereas spiking activity itself is not very metabolically demanding, events at the synapse are highly metabolically demanding

(Arthurs and Boniface 2002). These include re-establishment and maintenance of membrane potentials by active ion transport and glutamate reuptake by astrocytes (Magistretti and Pellerin 1999).

However, it may be important to note that although in the Logothetis et al study LFPs provided a better predictor of BOLD signal in certain cases, there was nevertheless a significant correlation between spiking activity and the haemodynamic response (Logothetis *et al.* 2001). In addition, the LFP includes contributions both from subthreshold potentials and from spiking activity. Therefore spiking activity *is* reflected in the BOLD signal, but cannot fully predict the signal. On the other hand, the correlation between firing output and BOLD may simply reflect the fact that firing output will be correlated somewhat with input strength.

3.1.5.3 Magnitude of response

A positive correlation between blood flow and blood oxygenation has been shown by simultaneous BOLD and perfusion imaging during presentation of alternating visual checkerboards (Zhu *et al.* 1998). Activation in V1 voxels that were suprathreshold by both techniques showed correlated increases in CBF and BOLD in response to increasing checkerboard frequency.

Consistent with the correlation between BOLD and local field potentials described above (Logothetis *et al.* 2001), BOLD is also positively correlated with population level electrical activity, as measured by somatosensory evoked potentials (SEP) after electrical stimulation of the median nerve (Arthurs *et al.* 2000). Increases in stimulation intensity led to correlated increases in BOLD and SEP amplitude.

3.1.6 Image Analysis

This section provides a brief overview of the steps required to move from the raw FMRI data to statistical maps of activated brain regions. FMRI data is noisy and therefore preprocessing steps are applied to minimise artefacts. After preprocessing, statistical analysis is carried out to determine which voxels are significantly activated.

3.1.6.1 Preprocessing of FMRI data

Motion correction: During the course of an FMRI experiment there will be movement of the brain within the imaged space due to physiological factors such as cardio-respiratory cycle, and to subject motion. The result of this is that the signal from an individual voxel may not correspond to the same point in the brain throughout the experiment. There are various methods for correcting for head motion. In the experiments presented in this thesis linear image registration techniques are used to align all volumes from an experiment with a single volume (Jenkinson and Smith 2001; Woods *et al.* 1999). The techniques employed here assume that head motion is a rigid body process. This means that the head can change its position and size but not its shape (estimation of changes in shape require non-linear registration techniques which are computationally demanding). The affine transformation techniques employed here estimate head movement with 12 parameters: translation, rotation, scaling and skew on the x, y and z axes.

Spatial smoothing: The main reason for spatially blurring FMRI data is to increase the signal to noise ratio. If noise varies randomly from voxel to voxel then spatially smoothing should cancel out noise. By contrast, if activation is larger than the size of the chosen smoothing kernel then activation should not be cancelled out to the same extent as noise. Therefore, if

small areas of activation are expected then minimal or no spatial smoothing should be carried out. In the experiments presented in this thesis spatial smoothing has been carried out with a Gaussian kernel of 5x5x5mm full width at half maximum. This kernel is only slightly larger (in plane) than the voxel size of 4x4x6mm. Therefore minimal smoothing was chosen for the experiments presented here. A second reason for spatial smoothing is that later clustering steps use Gaussian random field theory which assumes that the data is spatially smooth

Intensity normalisation: During the course of an experiment, there may be drifts in the overall level of signal (e.g due to temperature changes affecting scanner hardware). This drifting baseline can be corrected by intensity normalisation (i.e. rescaling of all voxel intensities (within a volume) by the same amount so that all volumes (over time) have the same mean intensity). However, this can lead to problems if strong activations are present. If a volume contains strong signal then it will have a high mean intensity and will be rescaled by a large factor and so non-activated regions in a strongly activated volume may begin to show up as deactivations. This potential problem, plus the fact that global intensity drifts are not expected to be substantial in FMRI (cf. PET, the technique for which this procedure was developed), means that intensity normalisation is often not a necessary, or even desirable step for FMRI analysis. Most of the experiments presented here have not employed intensity normalisation (exceptions are Sections 5 and 6). However, the data from each experiment (i.e. the entire time series) is scaled to have the same overall mean, so that subsequent group statistics are valid.

Temporal smoothing: There are two types of temporal smoothing that can be carried out on FMRI data – high pass and low pass. High pass filtering removes low frequency noise such as cardio-respiratory effects, or scanner-related drifts. The period of the high pass filter should be chosen so as not to remove variations that could be related to the experiment. In the studies presented here a filter of one and a half times the paradigm frequency has typically been used. Low pass filtering removes high frequency noise and can be analogous to spatial smoothing (described above) in that the aim is to cancel out random fluctuations due to noise while retaining genuine signal. However, by smoothing the signal in time (sometimes called 'precolouring') the temporal autocorrelation (i.e. similarity in signal between one time point and the next) is artificially increased and therefore the number of effectively independent timepoints is decreased. If this is not corrected for at later stages of statistical analysis then false positives can occur. An alternative approach involves estimating the amount of temporal smoothness in the data and removing this temporal autocorrelation during the statistical analysis stage (so called 'prewhitening') (Woolrich *et al.* 2001). Most of the experiments presented here have used prewhitening (except Sections 5 and 6).

3.1.6.2 Statistical analysis of single subject FMRI data

Statistical modelling: Once the data has been preprocessed the next step is to assess the degree to which the signal from different voxels corresponds to the task paradigm. There are a number of statistical approaches to quantifying this correspondence. A simple approach (employed in Sections 5 and 6) is to find the average signal during "on" blocks and the average signal during "off" blocks and compare them using a t-test. However, this approach ignores the temporal structure of the signal. The signal timecourse from each voxel can be compared to the timecourse of the paradigm (a simple box car) or to the expected

haemodynamic response (e.g the box car convolved with a haemodynamic response function such as a gaussian kernel). This can be done by simple correlation, or can be done within the framework of the general linear model (GLM, employed in Sections 4, 7, 8 and 9).

The experiments presented here use a univariate approach where each voxel is analysed separately at the model fitting stage. The model consists of separate explanatory variables (or regressors) that specify the timing of different types of events or blocks (e.g., tactile stimulation and visual stimulation). In the case of a single explanatory variable the GLM takes the simple form:

$$y = \beta x + e$$

where y is the data (over time) from a voxel, x is the model (i.e. the explanatory variable(EV)), β is the parameter estimate (the value by which x must be multiplied to give y – i.e the height of the signal response for that voxel) and e is the error in model fitting.

Parameter estimates therefore give an estimate of the amplitude of the response in a particular condition (and can be converted to values such as percentage signal change). To generate a statistical parameter, such as a t value, the parameter estimate is divided by the standard error of the parameter estimate. Activation for different conditions (i.e. different explanatory variables) can also be compared directly to each other by performing contrasts of parameter estimates. For example to detect where activation for EV1 (e.g. attended touch) is greater than for EV2 (e.g. unattended touch) involves subtracting the parameter estimate for EV1 from that for EV2 and dividing by the standard error of this new estimate.

The model can also be used to assess non-linear interactions between conditions (e.g. Section 7). For example if visual and touch stimuli were applied with different, but overlapping time courses then a positive interaction term would identify areas where the

signal during visuo-tactile stimulation was greater than the sum of the signal during purely visual stimulation and the signal during purely tactile stimulation.

Statistical inference: Once a statistical parameter has been calculated for each voxel it is then necessary to decide which parameters represent significant activation. This process of statistical thresholding can be carried out in different ways. The statistical parameters assigned to each voxel are associated with a probability (p-value) which can be used directly for thresholding. However, as there are typically tens of thousands of voxels in the brain, thresholding at a conventional level of $p<0.05$ will lead to many false positives due to the problem of multiple comparisons. Bonferroni corrections for multiple comparisons (i.e. dividing the p-threshold by the number of voxels) would be overly conservative as voxels are not independent from each other (due to physiological smoothness, the point spread in the MR signal due to T2* decay and the smoothness imposed by spatial filtering). An alternative voxel-based thresholding approach makes use of Gaussian random field theory to estimate the smoothness of the statistical map in terms of the number of resolution elements, or 'resels'. Correction is then made on the basis of the number of resels (which is less than the number of voxels) and is therefore more lenient (this technique was employed in Section 5). A third approach, which has been employed in all other experiments presented here, takes into account the size of an activated cluster. This 'cluster detection' approach, which also uses Gaussian random field theory, first thresholds the statistical map (at an experimenter defined threshold, e.g. $Z>3.1$), then assigns the resulting clusters (which may be as small as a single pixel) a probability value which is based on the size of the cluster and the initial statistical threshold chosen. This technique is typically more sensitive than voxel-based resel

thresholding, and is arguably more physiological informed as activated regions are expected to extend over multiple voxels.

3.1.6.3 Multi-subject statistics

Often an FMRI experiment will aim to characterise brain activation patterns for a particular population or differences between populations. This will typically involve aligning the brains of individual subjects into a standard co-ordinate system. The most commonly used co-ordinate system is that provided in the brain atlas of Talairach and Tournoux (Talairach and Tournoux 1988). Statistical methods for assessing group activation include 'fixed effects' and 'random effects' analyses. Fixed effects analyses only consider within subject variance whereas random effect analysis additionally consider between subject variances. Random effects analyses are therefore more conservative, but present a more valid representation of results if conclusions are to be made about the population from which subjects were drawn (rather than about that specific group of subjects). The voxel-based group analyses carried out in experiments in this thesis all employ random effects analyses (Sections 4, 6, 7, 8, 9).

There are a number of caveats to the interpretation of FMRI group analyses. Firstly, although template systems can provide a useful means of comparing activation loci between studies, it is important to note that different template images (eg the MNI template versus the Talairach template) are differently shaped. This means that an anatomical region will not necessarily occupy the same co-ordinates in the two systems.

Group analyses are strict tests as they require not only that a large proportion of subjects show an effect in a particular anatomical region but also that the voxels showing the effect overlap once the individual brains have been co-registered. This requirement might be

more easily met by large, diffuse areas of activation (see chapter 6 for further discussion of this point).

An alternative to voxel-based group analyses is a volumes of interest (VOI) approach. With this technique anatomically-defined VOIs are drawn on individual high-resolution scans. Statistics are then computed within VOIs, without the requirement that the VOIs from different subjects overlap in standard brain space. This technique has been used in addition to a voxel-based analysis in many of the experiments in this thesis.

3.1.7 Methodological issues

Having outlined some of the general principles of FMRI acquisition and analysis above, the following section deals further with specific methodological issues relevant to the experiments in this thesis. This section explains the rationale behind the particular approaches taken and decisions made in relation to experimental design and analysis.

3.1.7.1 Scanning patients – matching and monitoring performance

FMRI investigation of recovery of function in stroke will almost inevitably involve scanning patients during performance of a recovering, or recently recovered function. This raises the crucial issue of ensuring that affected task performance is comparable to whatever constitutes control task performance (e.g. movement of an unaffected limb or limb movement in a healthy control group). This issue is not simple and depends on the feature of the task that is of interest. In the motor system for example, a comparison could be made between movements which share the same absolute movement parameters (e.g. rate, amplitude) or between movements which require the same degree of effort (e.g. performing

at a percentage of maximum rate, amplitude etc). The choice of approach depends on the research question and both have been used in this thesis.

In section 4 stroke patients are compared to normal controls during performance of a hand-tapping task. Also, affected limb movement is compared to unaffected limb movement. For this experiment all subjects performed that task at a percentage of maximum tapping rate as the crucial question was whether motor system recruitment in patients was altered even if they found the task equally difficult as controls. In Section 8 stroke patients were investigated serially before and after a rehabilitation intervention. In this longitudinal design each individual patient effectively acted as his or her own control. For this experiment the rate and force of flexion-extension movements was individually set for each patient on the first testing session. However, over the course of the study these parameters did not change within an individual. This allowed assessment of whether motor system recruitment changed over time to enable individuals to produce the same absolute movement before or after therapy.

If interpretation of results from these studies rests on the aspects of performance that are being controlled or modulated then it is crucial that performance is monitored in some way. Methods for monitoring motor performance vary considerably in the literature, ranging from simple visual observation to preliminary attempts to record EMG in the magnet. Similarly, attempts to monitor motor performance vary somewhat through this thesis from visual observation (Sections 4 and 5) to recording button press responses (Sections 6,7,9) and force output (Section 8). Having an objective performance measure is hugely beneficial as it not only allows one to monitor accuracy and compliance but can also provide a continuous, quantitative measure which can then be fed into the FMRI analysis to identify areas whose activation is related to a particular movement parameter. Experiments

in this thesis have used performance measures only in the more limited sense of providing an indicator of accuracy and overall performance. However, technological advances in MR-compatible movement monitoring devices have introduced the possibility of more sophisticated routine monitoring (Liu *et al.* 2000)

3.1.7.2 Cross-sectional versus longitudinal designs

Imaging recovery in patient populations can be carried out with either a longitudinal or a cross-sectional approach. In a cross-sectional study patients are investigated at a single time point and differences can be identified between patients and controls, or between affected and unaffected tasks in patients (e.g. Section 4). Additionally, patterns of activation in patients can be correlated with functional scores. Longitudinal studies involve serial investigation of patients at different time points and can detect dynamic changes that occur over the course of recovery, or before and after therapeutic intervention (e.g. Section 8).

Longitudinal studies have increased power as they rely on within-subject comparisons. By contrast, cross-sectional studies often involve large amounts of between subject variability. However, longitudinal studies do have other problems such as the possible confounding effects of time. These include task practice and increasing familiarity with the experimental set-up.

3.1.7.3 Reproducibility and quantitation

Another important methodological choice is how to quantify FMRI data. Commonly reported activation measures include statistical parameters such as z scores or correlation coefficients, number of suprathreshold voxels, percent signal change and relative measures such as a laterality index (e.g. (C-I)/(C+I), where C=number of contralateral suprathreshold voxels and I=number of ipsilateral suprathreshold voxels). Activation quantitation provides

a means for comparing not only the location but also the magnitude of activation between groups, individuals, conditions, sessions and studies.

For longitudinal studies the reproducibility of the chosen measure is crucial. For example, to make conclusions about dynamic recovery processes it is desirable that changes in an activation measure over time can be related to meaningful recovery-related changes. However, it is known that changes in activation measures over time occur even in a normal subject performing the same task in repeated sessions, when few meaningful changes are expected (McGonigle *et al.* 2000). There are many potential contributors to this 'session effect'. These include physiological, psychological and hardware factors. Physiological factors include what the subject has eaten or drunk, time of day, drugs and tiredness. Psychological factors include boredom or practice effects. Scanner issues may include variations in hardware performance or the quality of pre-scanning steps. Some of these factors can be controlled for (e.g. time of day, food and drink) and others are less controllable (e.g. hardware performance). The choice of activation measure can also affect reproducibility. There is evidence to suggest that measures of signal change are more stable than values based on statistical parameters (e.g. z statistic, voxel counts), and that relative measures (e.g. laterality index) can be more stable than absolute measures. The arguments for these differences in stability are presented below.

Statistical parameters such as z or t statistics or correlation coefficients are essentially measures of an estimate of signal change divided by the error in the estimate. The number of voxels above an arbitrary statistical threshold will also depend on these values. Such measures therefore reflect the noise in signal measurements as much as the amplitude of signal change. Empirically, suprathreshold voxel counting has been shown to be highly unstable compared to measures of signal change. For example, in a visual task

suprathreshold voxel counts had a standard deviation of 74% across trial and subjects compared to less than 14% for a measure of signal change (Cohen and DuBois 1999). Another study found that for motor and visual tasks the number of suprathreshold voxels varied by up to 1150% whereas activation amplitude varied by up to 250% (Waldvogel *et al.* 2000). Similarly, a reproducibility study of active and passive movement found between session changes were apparent in activation volumes but not in the peak activation intensity (Loubinoux *et al.* 2001). Furthermore, by simulating data with different contrast-to-noise ratios (CNR), it was established that the correlation coefficient is highly dependent on CNR whereas signal change amplitude is not (Cohen and DuBois 1999).

There can also be differences in reproducibility and stability of absolute versus relative activation measures. An absolute measure, such as the number of suprathreshold voxels or the percent signal change, is highly dependent on experimental power and sensitivity. Factors affecting sensitivity include magnetic field strength as higher field magnets have greater signal to noise. Sensitivity may also depend on the duration of the experiment; statistical power will increase with an increasing number of measurements, up to a plateau (though if an experiment is over-long other factors such as fatigue or boredom will come into play). Sensitivity can additionally be affected by preprocessing steps such as the type of motion correction or temporal or spatial filtering applied to the data. Therefore, if comparisons are to be made between studies or timepoints, a relative measure, such as a laterality index, may prove more suitable than an absolute measure such as voxel counts.

3.1.7.4 Paradigm design and efficiency

Paradigm design for functional imaging studies has become increasingly sophisticated in recent years and experimenters are now faced with numerous decisions regarding how best

to design an experiment to answer a specific research question. One choice concerns timing of tasks or stimuli, with the principle decision to be made between a "block design" and an "event-related design" (Figure 3.8). A second choice concerns the method for identifying brain activation specific to the variable of interest. Options here include subtraction, parametric or conjunction designs.

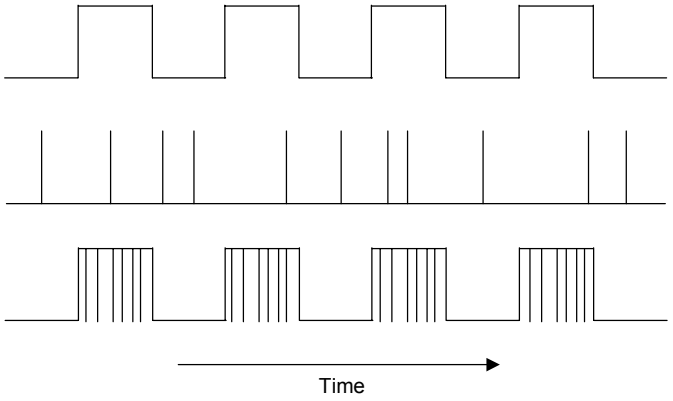

Figure 3.8: Paradigms can be presented in a block design (top) where tasks are presented in alternating epochs. Alternatively, tasks can be presented in an event-related design (middle) where single trials are presented intermittently throughout the experiment. It is also possible to combine these two approaches by presenting intermittent single trials, but in blocks of different types (bottom).

Deciding between options requires careful consideration of psychological, physiological and statistical issues specific to the question and population of interest. For example, a long duration event-related experiment involving rapid performance of a complex task would be powerful and appropriate for extracting the timing of subtle cognitive processes in groups of high functioning young subjects. However, such a design may not be appropriate for studying a simple sensory or motor function in a group of brain-damaged subjects who may not be able to cope with rapid task performance or long periods of time in the scanner.

Different designs also vary in 'efficiency'. This measure reflects the accuracy with which activations can be estimated in a given scanning time. The most efficient design is a conventional block design (Friston *et al.* 1999).

All experiments in this thesis use a conventional block design with 24-30 second task blocks alternating with rest blocks. A number of factors influenced this choice. Firstly the high efficiency of these designs which allows scanning runs to be short. This was considered to be particularly important for patient studies as the amount of time that the subjects were able to tolerate being in the scanner, and remain still and focussed on the task was limited. It is important to limit discomfort as much as possible in order to maximise the subjects' well-being, the quality of the data, and the likelihood of persuading subjects to come back again in the case of longitudinal studies. The analysis of block designs can also be simpler, and less susceptible to reduced sensitivity due to inaccuracies in event timing or specification of the haemodynamic response function.

However, choosing block designs does forfeit some of the advantages associated with event-related designs. These include the ability to characterise accurately the haemodynamic response to single events with high temporal resolution (Buckner 1998). This could be of particular interest in studies of stroke, as there is evidence that the shape of the haemodynamic response over a block is altered in patients with subcortical stroke (Pineiro *et al.* 2002). It would be interesting to characterise these differences with the greater temporal resolution offered by event related FMRI.

Another disadvantage of block designs is the lack of control over the cognitive state of the subject during long periods of 'rest'. One study which contrasted activation during rest with activation during perceptual task blocks found relatively increased activity in language-related areas during rest, suggesting that subjects engage in active semantic, conceptual or linguistic processing during rest blocks when they are not being occupied by any other tasks (Binder *et al.* 1999).

3.2 Transcranial Magnetic Stimulation (TMS)

Use of Transcranial Magnetic Stimulation (TMS) has accelerated considerably since the first successful demonstration of human brain stimulation by magnetic fields by Barker in 1985 (Barker *et al.* 1985). In recent years application of TMS as a 'virtual lesion' technique has proved particularly powerful in the field of cognitive neuroscience. The following sections describe the principles behind TMS and methodological and safety issues which should influence the design of TMS experiments.

3.2.1 Principles of TMS

TMS is based on Faraday's principle of electromagnetic induction (for review see (Walsh and Cowey 2000)). Faraday demonstrated that an electrical current flowing through a coil of wire generates a time-varying magnetic field which in turn induces an electrical current in a second coil of wire. In a TMS experiment the second coil is replaced by the human cortex. A stimulating coil is held over the scalp and a large very rapidly changing current is passed through the coil, generating a changing magnetic field that induces an electrical current in the underlying cortex (Figure 3.9; for reviews see (Mills 1999; Walsh and Rushworth 1999).

Unlike electrical fields, magnetic fields are hardly attenuated as they pass through the skull. The size of the induced tissue current is dependent on the amplitude and the rate of change of the current in the stimulating coil. To achieve this rapid rate of change a TMS pulse typically has a short rise time (about 200μs) and an overall duration of about 1 millisecond. If large enough, the induced tissue current can stimulate neurons or change the resting membrane potential.

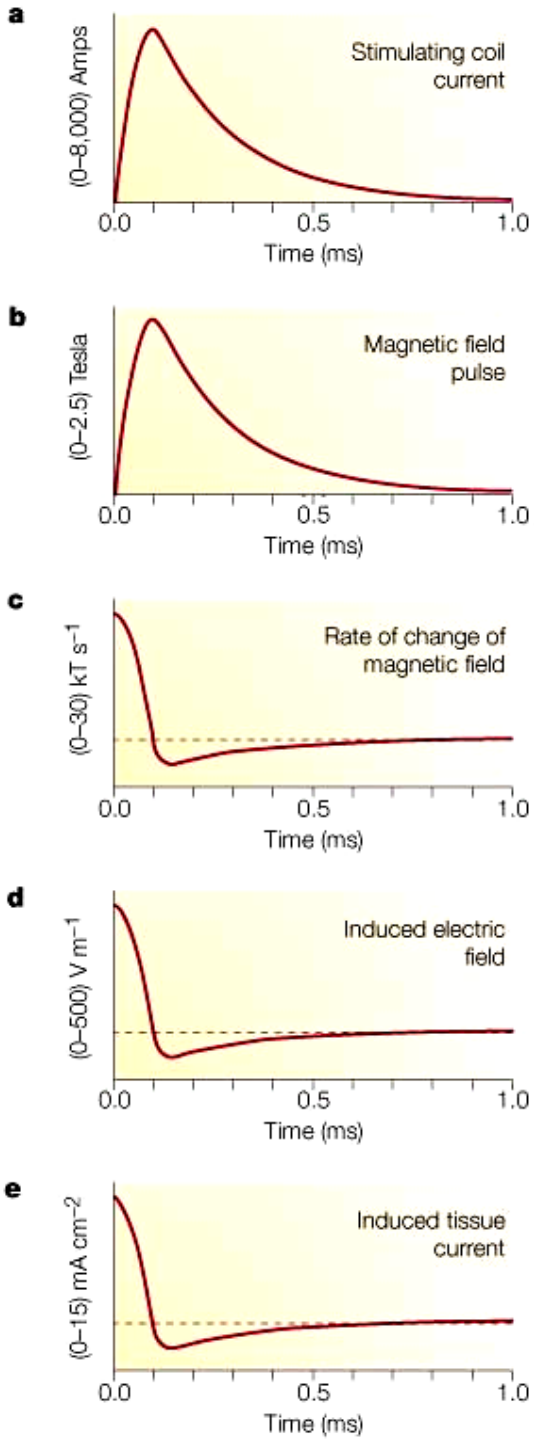

Figure 3.9 Sequence of events that occur with a single TMS pulse. A rapidly changing electrical current of up to 8kA is passed through the coil (a) inducing a magnetic field of up to 2.5T (b) that has a very steep rate of change (c) and so generates an electrical field (d) that induces a current in the underlying tissue. Figure adapted from the Magstim Company Guide to Magnetic Stimulation for Walsh and Cowey (2001)

TMS can be used to stimulate output from a cortical area. Applied locally over primary motor cortex TMS can evoke a muscle response. Applied over primary visual cortex TMS can elicit visual phosphenes. However, TMS can also be used as a disruptive technique (discussed further in Section 3.2.2). In studies of primary visual cortex Amassian and colleagues found that TMS pulses below the threshold for phosphenes were capable of transiently disrupting visual perception (Amassian *et al.* 1989; Maccabee *et al.* 1991). Similarly, TMS of primary motor cortex after a cue to move can slow movements (Day *et al.* 1989). This slowing effect is greatest when TMS is applied just before the expected movement time (Ziemann *et al.* 1997).

These effects are due to the fact that TMS simultaneously stimulates large populations of neurons and therefore effectively introduces noise to a cortical area. If a region is processing a structured, task-relevant signal at the time that a TMS pulse is delivered, then the TMS pulse will temporarily and locally reduce the signal to noise ratio. The extent to which the signal to noise ratio is reduced (depending on the amplitude and duration of TMS, and the size of the original cortical signal) determines whether and to what extent the TMS pulse has an observable behavioural effect.

The mechanisms of action of TMS remain unclear. There is debate over which neuronal populations are affected by TMS, the depth to which TMS infiltrates, and the degree to which interconnected regions are affected by stimulation of a single cortical site. The immediate effect of TMS is to produce synchronous activity (i.e. noise) in underlying neurons. This causes release of prolonged GABAergic IPSPs that inhibit subsequent activity for 50-250ms. When motor cortex is stimulated this pattern is reflected by an initial MEP followed by a silent period during which further TMS pulses are ineffective (Fuhr *et al.* 1991; Kujirai *et al.* 1993). The duration of the silent period evoked by TMS is correlated with the

amount of reaction time slowing with motor cortex TMS, suggesting that the two effects may be mediated by a common inhibitory mechanism (Ziemann *et al.* 1997).

Coil orientation affects the neural elements that are activated by TMS. This is because of variations in the orientation of the induced electrical current, and variation in the orientation of different cell types in the cortex. For example, currents that flow in an anterior-posterior direction across the central sulcus evoke EMG responses 2-3ms longer than currents flowing in the opposite direction (Day *et al.* 1989). Computer models suggest that TMS-induced currents flow parallel to the brain surface (Tofts 1990). As neurons are more effectively excited by transverse rather than longitudinal currents this will selectively stimulate cells that are oriented perpendicular to the brain surface (Jahanshahi and Rothwell 2000). The most effective orientation for stimulating intrinsic hand muscles with a figure-of-eight coil is 50° from the parasaggital plane with a backward flowing inducing current (Mills *et al.* 1992). This orientation would induce a tissue current flowing forwards at approximately right angles to the central sulcus. Mills et al (1992) suggest that such a current would preferentially excite horizontal fibre systems which are aligned in this direction.

Despite ongoing uncertainty about the precise neuronal effects of TMS, there is consensus that the functional effects of a TMS pulse are to introduce electrical noise to the underlying cortex. In this way TMS can be seen as a temporary, or virtual, lesion technique.

3.2.2 TMS as a virtual lesion technique

When employed as a virtual lesion technique TMS is unique among methods for studying the human brain. The lesion technique in experimental animals has proved invaluable for providing information on which brain areas are necessary for performance of a given task. The closest approximation to this approach in humans has been the investigation of brain-

damaged patients. However, damage due to trauma or stroke is often extensive and rarely restricted to a specific functional-anatomical unit. TMS occupies a unique location in what has been described as the cognitive neuroscience "problem space" (Figure 3.10). It potentially has a spatial resolution of less than a centimetre (Section 3.2.2.1), a temporal resolution of a few milliseconds (Section 3.2.2.2), and the crucial additional feature of enabling interference with processing. TMS can therefore be used to determine where and when necessary cortical processing occurs for a given task.

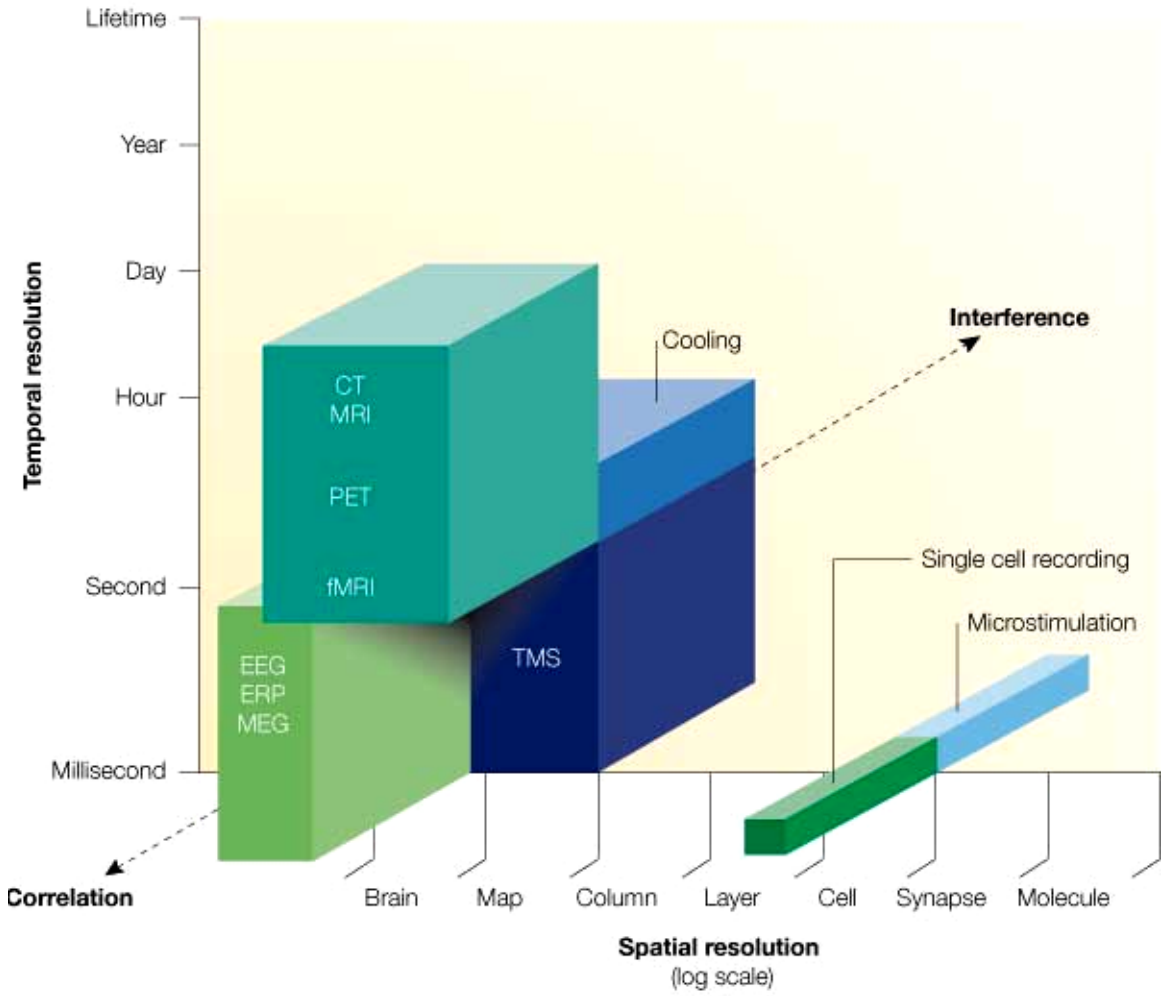

Figure 3.10: 'Problem space' of cognitive neuroscience techniques. TMS has a similar spatial resolution to human brain imaging methods and a similar temporal resolution to ERPs. TMS occupies a unique spot in the problem space as it has the additional feature of being able to transiently interfere with processing, whereas human imaging techniques provide only correlative information. Figure from Walsh and Cowey (2001)

3.2.2.1 Spatial resolution

Early TMS experiments were performed with circular coils (Figure 3.11). Circular coils produce diffuse magnetic fields that can be useful for inducing effects over a wide cortical area. However, to stimulate a spatially restricted area of cortex circular coils are unsuitable and have been largely replaced by figure-of-eight coils (Figure 3.11). Figure-of-eight coils consist of adjoining circular wire windings. Both circles produce diffuse fields but at the intersection the fields summate to produce a clear peak (Figure 3.11).

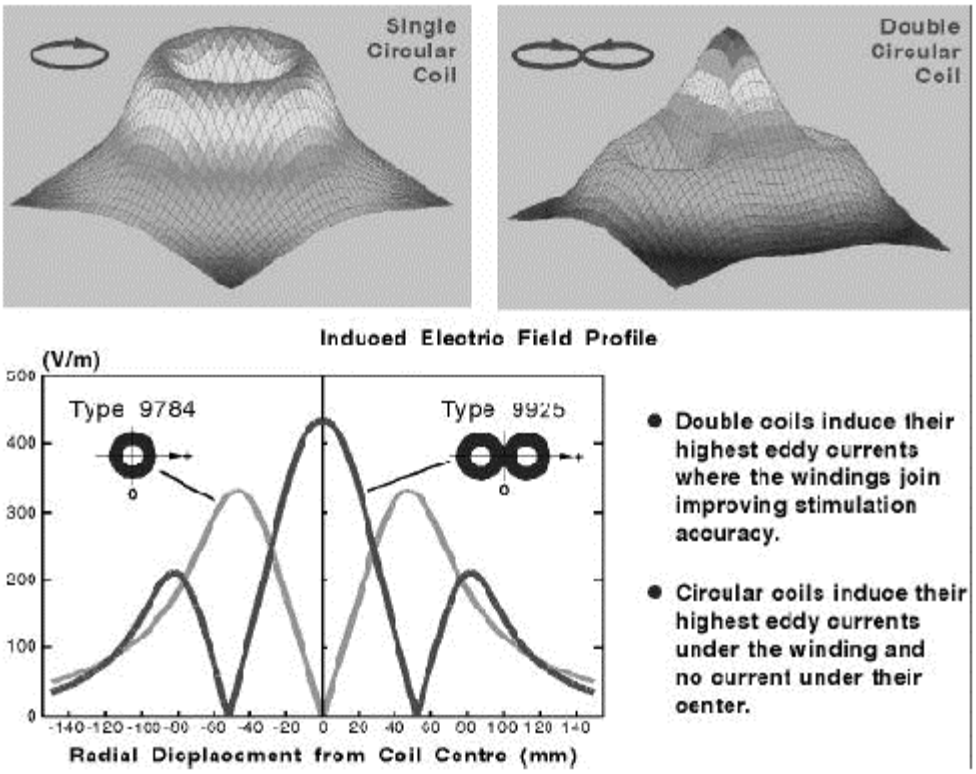

Figure 3.11: Induced electrical fields for circular and figure of eight coils. For a circular coil the field is maximal underneath the windings. For a figure of eight coil the field underneath the windings of the two circles summates at their intersection to produce a localised peak. Figure from the Magstim Company Guide to Magnetic Stimulation.

Although one can localise the peak of the magnetic field under the coil, there remains scepticism over the spatial resolution of TMS given the demonstration of current spread to adjacent and interconnected cortical regions (Figure 3.12). Spreading effects of

TMS can occur because of physical reasons (i.e. spread of the induced field through the tissue) or physiological reasons (i.e. trans-synaptic current transmission) Following a single pulse over primary motor cortex, there is electrical activity directly under the coil after 3 ms, in adjacent cortical regions after 10ms, and in homologous regions of the opposite hemisphere after 24ms (Ilmoniemi *et al.* 1997). However, despite the fact that TMS-induced current can spread, it remains possible to pinpoint the time and place where current is maximum, i.e. directly under the intersection of the figure of eight, a few milliseconds after the pulse. Provided one applies pulses close to the threshold for inducing a behavioural effect, this allows sufficient functional-spatial resolution as the diffuse current will not have a detectable, behaviourally-relevant effect.

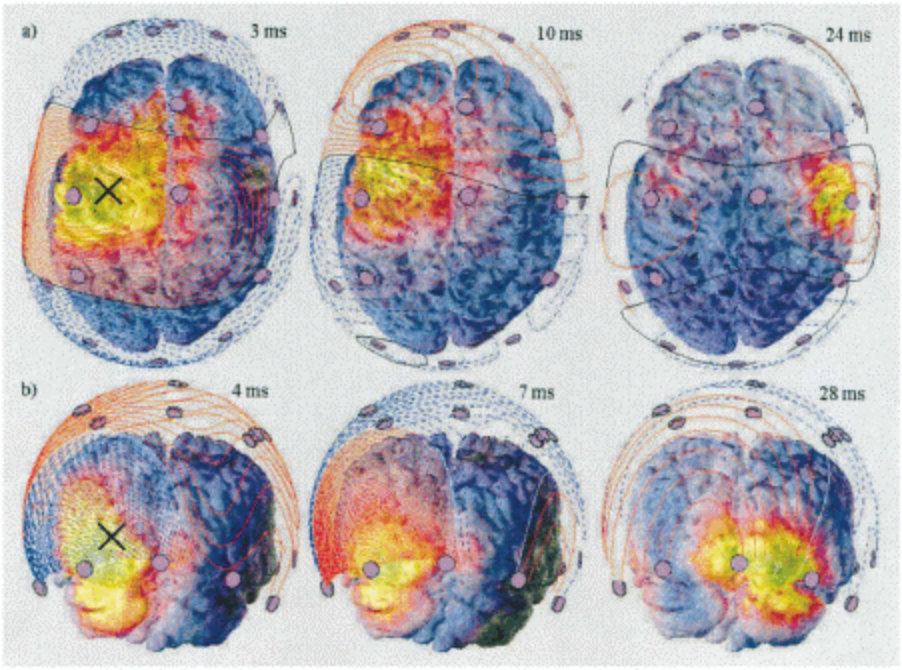

Figure 3.12: Spread of electrical activity as measured by EEG after a single TMS pulse (at location marked X) to motor cortex (top) or visual cortex (bottom). Figure from (Ilmoniemi *et al.* 1997)

In practice, studies have produced functionally-dissociable effects from scalp sites as little as a centimetre apart. For example, stimulating different sites over motor cortex, it is

possible to localise "hot spots" for stimulation of individual forearm and hand muscles that are separated by a centimetre (Wassermann *et al.* 1992). In a study using TMS as a virtual lesion technique, Schluter et al produced dissociable patterns of slowing of reaction times from stimulating sites 1.5cm apart, corresponding to primary and premotor cortex (Schluter *et al.* 1998).

3.2.2.2 Temporal resolution

TMS can be applied as single pulses or as trains of pulses (repetitive TMS, rTMS). Although a single TMS pulse can last only one millisecond, its effect on underlying and interconnected cortex can have a much longer duration. A single pulse of TMS produces activation detectable by electroencephalography (EEG) for up to 30ms (Figure 3.12). However, long lasting decaying TMS-induced activity may not be strong enough to have any effect on the task. The relevant temporal resolution of the technique can be determined from the degree to which single TMS pulses separated in time can have functionally-dissociable effects. A number of studies have used single pulse TMS to extract the timing of cortical processing. For example, in Schluter et al's study of motor and premotor areas, PMC stimulation slowed responses when applied in an early time window (about 140ms after a cue to move) whereas MC stimulation was effective 40ms later (Schluter *et al.* 1998). Ashbridge et al applied TMS during 'pop-out' or conjunction visual search tasks. TMS was applied over the parietal cortex at timepoints 20 to 200ms (separated by 20ms) after the search array appeared. Parietal TMS slowed reaction times on a conjunction search task (and not on pop-out search) when applied 100ms after the onset of the search array for target present trials, and 160ms after the array onset for target absent trials (Ashbridge *et al.* 1997).

TMS can be used to investigate the relative timing of processing in different brain areas. Pascual-Leone and Walsh used used two coils to separately stimulate primary visual cortex (V1) and the visual motion area (V5) to investigate the role of back-projections from V5 to V1 (Pascual-Leone and Walsh 2001). V5 was stimulated above phosphene threshold whereas V1 was stimulated below threshold. V5 stimulation therefore evoked moving phosphenes whereas TMS over V1 temporarily interfered with local processing. Disrupting V1 activity before V5 stimulation had no effect on perception of phosphenes. However, disrupting V1 activity 5 to 45ms after V5 stimulation abolished or reduced the sensation of visual motion, suggesting that fast backprojections from V5 to V1 are important for visual motion perception.

The timing of task disruption by TMS corresponds well to the time when an area begins to be active in single unit recording studies. The 140ms time point in the study by Schluter et al is the time at which 20% of dorsal premotor cortex neurons are active in a movement selection task (di Pellegrino and Wise 1991). By contrast, peak activation times reported by event-related potential (ERP) or magnetoencephalography (MEG) studies tend to be later than critical time windows for TMS (Walsh and Rushworth 1999). This might reflect the fact that ERP and MEG signals reflect the build up of population level neuronal activity. It appears that TMS will be most effective if applied at the beginning of this build up rather than when it has neared its peak.

3.2.3 Methodological considerations

The following section outlines some of the methodological issues specific to the TMS experiments in this thesis.

3.2.3.1 Single pulse or repetitive TMS

The two approaches of single or repetitive pulse TMS have different strengths and weaknesses. Repetitive TMS (rTMS) will disrupt processing over a longer time period. It is therefore less likely that an effect in an area will be missed due to stimulating at the wrong time. However, as a result rTMS can tell us little about the timing of events. With single pulse TMS it is possible to determine the timing of cortical processing by producing functionally-dissociable effects from pulses separated in time (see Section 3.2.1.2). However, the behavioural effects of single pulses of TMS will be more subtle, and more dependent on the pulses being applied at the critical time point.

3.2.3.2 Safety and side-effects

The primary safety concern with TMS is the risk of increased electrical activity inducing seizures. In general, this concern is restricted to rTMS, although with patient populations there is a potential risk even with single pulse TMS. Although there have been cases of rTMS-induced seizures in normal subjects there have been a number of safety studies of the technique which have established working guidelines within which seizures have never been induced in normal subjects without a personal or family history of epilepsy (Pascual-Leone *et al.* 1993; Wassermann 1998).

There are fewer safety issues surrounding single pulse TMS. Safety or side-effect concerns include hearing impairments, hormonal changes, mood changes and cognitive changes (Cracco *et al.* 1999). Studies of serum prolactin, ACTH and cortisol levels have not

shown any changes after single pulse TMS, there is no evidence for long term cognitive effects and magnetic, electrical and thermal energy levels in the brain during single pulse TMS are within safe limits based on accepted clinical procedures (Cracco *et al.* 1999).

There have been no reports of single pulse TMS inducing seizures in neurologically normal subjects without a personal or family history of epilepsy. Homberg and Netz (1989) reported a patient with a large ischemic scar who had a first seizure probably induced by TMS (Homberg and Netz 1989). However, this was an isolated case in a group of 700 investigations including 150 patients with hemispheric stroke. Kandler (1990) reported that in 800 TMS investigations including 76 in stroke patients no seizures were observed during testing (Kandler 1990). Convulsions did develop in two patients with multiple sclerosis (MS) within a month of TMS but this was within the normal prevalence rate for MS. There have been no other reports of seizures induced by TMS in stroke patients, despite its use on hundreds of subjects. The TMS experiments in this thesis used only single pulse TMS. The frequency and intensity of stimulation used was well within the recommended limits (Wassermann 1998)

There are no clear adverse short or long-term effects of single pulse TMS on cognition or mood (Cracco *et al.* 1999). Performance on a variety of psychometric tests was not impaired immediately after a short session of single pulse TMS or at a one-year follow up (Bridgers 1991). However, the fact that rTMS of prefrontal cortex can improve mood in depressed patients demonstrates that long-term effects are possible in certain populations and with certain stimulation sites and parameters (Pascual-Leone *et al.* 1996).

References

Aguirre, G. K., Zarahn, E., and D'Esposito, M. (1998) The variability of human, BOLD hemodynamic responses. *Neuroimage* **8,** 360-369.

Amassian, V. E., Cracco, R. Q., Maccabee, P. J., Cracco, J. B., Rudell, A., and Eberle, L. (1989) Suppression of visual perception by magnetic coil stimulation of human occipital cortex. *Electroencephalogr Clin Neurophysiol* **74,** 458-462.

Arthurs, O. J. and Boniface, S. J. (2002) How well do we understand the neural basis of the BOLD signal? *Trends Neurosci.*

Arthurs, O. J., Williams, E. J., Carpenter, T. A., Pickard, J. D., and Boniface, S. J. (2000) Linear coupling between functional magnetic resonance imaging and evoked potential amplitude in human somatosensory cortex. *Neuroscience* **101,** 803-806.

Ashbridge, E., Walsh, V., and Cowey, A. (1997) Temporal aspects of visual search studied by transcranial magnetic stimulation. *Neuropsychologia* **35,** 1121-1131.

Bandettini, P. A. (1999) The temporal resolution of functional MRI. In: *Functional MRI*, pp. 195-204. Eds C. Moonen, P. A. Bandettini. Springer: Berlin.

Barker, A. T., Jalinous, R., and Freeston, I. L. (1985) Non-invasive magnetic stimulation of human motor cortex. *Lancet* **1,** 1106-1107.

Belliveau, J. W., Kennedy, D. N., Jr., McKinstry, R. C., Buchbinder, B. R., Weisskoff, R. M., Cohen, M. S., Vevea, J. M., Brady, T. J., and Rosen, B. R. (1991) Functional mapping of the human visual cortex by magnetic resonance imaging. *Science* **254,** 716-719.

Binder, J. R., Frost, J. A., Hammeke, T. A., Bellgowan, P. S., Rao, S. M., and Cox, R. W. (1999) Conceptual processing during the conscious resting state. A functional MRI study. *J Cogn Neurosci* **11,** 80-95.

Bridgers, S. L. (1991) The safety of transcranial magnetic stimulation reconsidered: evidence regarding cognitive and other cerebral effects. *Electroencephalogr Clin Neurophysiol Suppl* **43,** 170-179.

Buckner, R. L. (1998) Event-related fMRI and the hemodynamic response. *Hum Brain Mapp* **6,** 373-377.

Buxton, R. B., Wong, E. C., and Frank, L. R. (1998) Dynamics of blood flow and oxygenation changes during brain activation: the balloon model. *Magn Reson Med* **39,** 855-864.

Cohen, M. S. and DuBois, R. M. (1999) Stability, repeatability, and the expression of signal magnitude in functional magnetic resonance imaging. *J Magn Reson Imaging* **10,** 33-40.

Cracco, R. Q., Cracco, J. B., Maccabee, P. J., and Amassian, V. E. (1999) Cerebral function revealed by transcranial magnetic stimulation. *J Neurosci Methods* **86,** 209-219.

Day, B. L., Dressler, D., Maertens, d. N., Marsden, C. D., Nakashima, K., Rothwell, J. C., and Thompson, P. D. (1989) Electric and magnetic stimulation of human motor cortex: surface EMG and single motor unit responses. *J Physiol* **412,** 449-473.

di Pellegrino, G. and Wise, S. P. (1991) A neurophysiological comparison of three distinct regions of the primate frontal lobe. *Brain* **114 (Pt 2),** 951-978.

Duong, T. Q., Kim, D. S., Ugurbil, K., and Kim, S. G. (2000) Spatiotemporal dynamics of the BOLD fMRI signals: toward mapping submillimeter cortical columns using the early negative response. *Magn Reson Med* **44,** 231-242.

Friston, K. J., Zarahn, E., Josephs, O., Henson, R. N., and Dale, A. M. (1999) Stochastic designs in event-related fMRI. *NeuroImage* **10,** 607-619.

Fuhr, P., Agostino, R., and Hallett, M. (1991) Spinal motor neuron excitability during the silent period after cortical stimulation. *Electroencephalogr Clin Neurophysiol* **81,** 257-262.

Gati, J. S., Menon, R. S., Ugurbil, K., and Rutt, B. K. (1997) Experimental determination of the BOLD field strength dependence in vessels and tissue. *Magn Reson Med* **38,** 296-302.

Gjedde, A. (1997) The relation between brain function and cerebral blood flow and metabolism. In: *Cerebrovascular Disease*, pp. 23-40. Eds H. Batjer, L. Caplan, L. Friberg, R. Greenlee, R. Kopitnik, W. Young. Lippincott-Raven: Philadelphia.

Hashemi, R. and Bradley, W. (1997) *MRI the basics*. Williams and Wilkins: Baltimore.

Homberg, V. and Netz, J. (1989) Generalised seizures induced by transcranial magnetic stimulation of motor cortex. *Lancet* **2,** 1223.

Hu, X., Le, T. H., and Ugurbil, K. (1997) Evaluation of the early response in fMRI in individual subjects using short stimulus duration. *Magn Reson Med* **37,** 877-884.

Ilmoniemi, R. J., Virtanen, J., Ruohonen, J., Karhu, J., Aronen, H. J., Naatanen, R., and Katila, T. (1997) Neuronal responses to magnetic stimulation reveal cortical reactivity and connectivity. *Neuroreport* **8,** 3537-3540.

Jahanshahi, M. and Rothwell, J. (2000) Transcranial magnetic stimulation studies of cognition: an emerging field. *Exp Brain Res* **131,** 1-9.

Jenkinson, M. and Smith, S. (2001) Global optimisation for robust affine registration. *Medical Image Analysis* **5,** 143-156.

Kandler, R. (1990) Safety of transcranial magnetic stimulation. *Lancet* **335,** 469-470.

Kim, D. S., Duong, T. Q., and Kim, S. G. (2000) High-resolution mapping of iso-orientation columns by fMRI. *Nat Neurosci* **3,** 164-169.

Kim, S. G., Lee, S. P., Goodyear, B. G., and Silva, A. (1999) Spatial resolution of BOLD and other FMRI techniques. In: *Functional MRI*, pp. 221-232. Eds C. Moonen, P. A. Bandettini. Springer: Berlin.

Kujirai, T., Caramia, M. D., Rothwell, J. C., Day, B. L., Thompson, P. D., Ferbert, A., Wroe, S., Asselman, P., and Marsden, C. D. (1993) Corticocortical inhibition in human motor cortex. *J Physiol* **471,** 501-519.

Lai, S., Glover, G. H., and Haacke, E. (1999) Spatial selectivity of BOLD contrast: Effects in and around draining veins. In: *Functional MRI*, pp. 221-232. Eds C. Moonen, P. A. Bandettini. Springer: Berlin.

Liu, J. Z., Dai, T. H., Elster, T. H., Sahgal, V., Brown, R. W., and Yue, G. H. (2000) Simultaneous measurement of human joint force, surface electromyograms, and functional MRI-measured brain activation. *J Neurosci Methods* **101,** 49-57.

Logothetis, N. K., Pauls, J., Augath, M., Trinath, T., and Oeltermann, A. (2001) Neurophysiological investigation of the basis of the fMRI signal. *Nature* **412,** 150-157.

Loubinoux, I., Carel, C., Alary, F., Boulanouar, K., Viallard, G., Manelfe, C., Rascol, O., Celsis, P., and Chollet, F. (2001) Within-session and between-session reproducibility of cerebral sensorimotor activation: a test--retest effect evidenced with functional magnetic resonance imaging. *J Cereb Blood Flow Metab* **21,** 592-607.

Maccabee, P. J., Amassian, V. E., Cracco, R. Q., Cracco, J. B., Rudell, A. P., Eberle, L. P., and Zemon, V. (1991) Magnetic coil stimulation of human visual cortex: studies of perception. *Electroencephalogr Clin Neurophysiol Suppl* **43,** 111-120.

Magistretti, P. and Pellerin, L. (1999) Regulation of cerebral energy metabolism. In: *Functional MRI*, pp. 25-34. Eds C. Moonen, P. A. Bandettini. Springer: Berlin.

Malonek, D. and Grinvald, A. (1996) Interactions between electrical activity and cortical microcirculation revealed by imaging spectroscopy: implications for functional brain mapping. *Science* **272,** 551-554.

Marrett, S., Fujita, H., Meyer, E., Ribeiro, L., Evans, A., Kuwabara, H., and Gjedde, A. (1993) Simulus specific increases of oxidative metabolism in human visual cortex. In: *Quantification of brain function: Tracer kinetics and image analysis in brain PET*, pp. 217-224. Eds K. Uemera, N. A. Lassen, T. Jones, I. Kanno. Elsevier: Amsterdam.

McGonigle, D. J., Howseman, A. M., Athwal, B. S., Friston, K. J., Frackowiak, R. S., and Holmes, A. P. (2000) Variability in fMRI: an examination of intersession differences. *NeuroImage* **11,** 708-734.

Menon, R. S. and Goodyear, B. G. (1999) Spatial and temporal resolution in fMRI. In: *Functional magnetic resonance imaging: Methods for neuroscience*, Eds P. Jezzard, P. M. Matthews, S. Smith. Oxford University Press: Oxford.

Menon, R. S., Ogawa, S., Hu, X., Strupp, J. P., Anderson, P., and Ugurbil, K. (1995) BOLD based functional MRI at 4 T includes a capillary bed contribution: echo-planar imaging correlates with previous optical imaging using intrinsic signals. *Magn Reson Med* **33,** 453-459.

Menon, R. S., Ogawa, S., Strupp, J. P., and Ugurbil, K. (1997) Ocular dominance in human V1 demonstrated by functional magnetic resonance imaging. *J Neurophysiol* **77,** 2780-2787.

Mills, K. R. (1999) Biophysics of magnetic stimulation. In: *Magnetic Stimulation of the Human Nervous System*, pp. 7-26. Oxford University Press: Oxford.

Mills, K. R., Boniface, S. J., and Schubert, M. (1992) Magnetic brain stimulation with a double coil: the importance of coil orientation. *Electroencephalogr Clin Neurophysiol* **85,** 17-21.

Nudo, R. J. and Masterton, R. B. (1986) Stimulation-induced [14C]2-deoxyglucose labeling of synaptic activity in the central auditory system. *J Comp Neurol* **245,** 553-565.

Ogawa, S., LEE, T. M., KAY, A. R., and Tank, D. W. (1990) Brain magnetic resonance imaging with contrast dependent on blood oxygenation. *Proc Nat Acad Sci (USA)* 9868-9872.

Ogawa, S., Menon, R. S., Tank, D. W., Kim, S. G., Merkle, H., Ellermann, J. M., and Ugurbil, K. (1993) Functional brain mapping by blood oxygenation level-dependent contrast magnetic resonance imaging. A comparison of signal characteristics with a biophysical model. *Biophys J* **64,** 803-812.

Pascual-Leone, A., Houser, C. M., Reese, K., Shotland, L. I., Grafman, J., Sato, S., Valls, S. J., Brasil, N. J., Wassermann, E. M., Cohen, L. G., and Hallett, M. (1993) Safety of rapid-rate transcranial magnetic stimulation in normal volunteers. *Electroencephalogr Clin Neurophysiol* **89,** 120-130.

Pascual-Leone, A., Rubio, B., Pallardo, F., and Catala, M. D. (1996) Rapid-rate transcranial magnetic stimulation of left dorsolateral prefrontal cortex in drug-resistant depression. *The Lancet* **348,** 233-237.

Pascual-Leone, A. and Walsh, V. (2001) Fast backprojections from the motion to the primary visual area necessary for visual awareness. *Science* **292,** 510-512.

Pineiro, R., Pendlebury, S., Johansen-Berg, H., and Matthews, P. M. (2002) Altered hemodynamic responses in patients after subcortical stroke measured by functional MRI. *Stroke* **33,** 103-109.

Rajapakse, J. C., Kruggel, F., Maisog, J. M., and von Cramon, D. Y. (1998) Modeling hemodynamic response for analysis of functional MRI time- series. *Hum Brain Mapp* **6,** 283-300.

Schluter, N. D., Rushworth, M. F., Passingham, R. E., and Mills, K. R. (1998) Temporary interference in human lateral premotor cortex suggests dominance for the selection of movements. A study using transcranial magnetic stimulation. *Brain* **121,** 785-799.

Segebarth, C., Delon-Martin, C., Belle, V., Roth, M., Massarelli, R., Lamalle, L., and Decorps, M. (1999) Functional MR angiography using in-flow and phase-contrast MR acquisition techniques. In: *Functional MRI*, pp. 83-88. Eds C. Moonen, P. A. Bandettini. Springer: Berlin.

Talairach, J. and Tournoux, P. (1988) *Co-planar stereotaxic atlas of the human brain*. Theime: Stuttgart.

Tofts, P. S. (1990) The distribution of induced currents in magnetic stimulation of the nervous system. *Phys Med Biol* **35,** 1119-1128.

Turner, R., Jezzard, P., Wen, H., Kwong, K. K., Le Bihan, D., Zeffiro, T., and Balaban, R. S. (1993) Functional mapping of the human visual cortex at 4 and 1.5 tesla using deoxygenation contrast EPI. *Magn Reson Med* **29,** 277-279.

Vanzetta, I. and Grinvald, A. (1999) Increased cortical oxidative metabolism due to sensory stimulation: implications for functional brain imaging. *Science* **286,** 1555-1558.

Villringer, A. (1999) Physiological changes during brain activaiton. In: *Functional MRI*, pp. 3-14. Eds C. Moonen, P. A. Bandettini. Springer: Berlin.

Waldvogel, D., van Gelderen, P., Muellbacher, W., Ziemann, U., Immisch, I., and Hallett, M. (2000) The relative metabolic demand of inhibition and excitation. *Nature* **406,** 995-998.

Walsh, V. and Cowey, A. (2000) Transcranial magnetic stimulation and cognitive neuroscience. *Nat Rev Neurosci* **1,** 73-79.

Walsh, V. and Rushworth, M. (1999) A primer of magnetic stimulation as a tool for neuropsychology. *Neuropsychologia* **37,** 125-135.

Wassermann, E. M. (1998) Risk and safety of repetitive transcranial magnetic stimulation: report and suggested guidelines from the International Workshop on the Safety of Repetitive Transcranial Magnetic Stimulation, June 5-7, 1996. *Electroencephalogr Clin Neurophysiol* **108,** 1-16.

Wassermann, E. M., McShane, L. M., Hallett, M., and Cohen, L. G. (1992) Noninvasive mapping of muscle representations in human motor cortex. *Electroencephalogr Clin Neurophysiol* **85,** 1-8.

Woods, R. P., Dapretto, M., Sicotte, N. L., Toga, A. W., and Mazziotta, J. C. (1999) Creation and use of a Talairach-compatible atlas for accurate, automated, nonlinear intersubject registration, and analysis of functional imaging data. *Hum Brain Mapp* **8,** 73-79.

Woolrich, M. W., Ripley, B. D., Brady, M., and Smith, S. M. (2001) Temporal Autocorrelation in Univariate Linear Modeling of FMRI Data. *NeuroImage* **14,** 1370-1386.

Zhu, X. H., Kim, S. G., Andersen, P., Ogawa, S., Ugurbil, K., and Chen, W. (1998) Simultaneous oxygenation and perfusion imaging study of functional activity in primary visual cortex at different visual stimulation frequency: quantitative correlation between BOLD and CBF changes. *Magn Reson Med* **40,** 703-711.

Ziemann, U., Tergau, F., Netz, J., and Homberg, V. (1997) Delay in simple reaction time after focal transcranial magnetic stimulation of the human brain occurs at the final motor output stage. *Brain Res* **744,** 32-40.